Electrochimica Acta 55 (2010) 5831–5839

Contents lists available at ScienceDirect

Electrochimica Acta

journal homepage: www.elsevier.com/locate/electacta

Hydrogenation of chalcones using hydrogen permeating through a Pd and palladized Pd electrodes

M. Gutierrez [a], M.A. Nazareno [a], V. Sosa [b], B.A. López de Mishima [a,*], H.T. Mishima [a]

[a] INQUINOA - CONICET, Instituto de Ciencias Químicas, Facultad de Agronomía Agroindustrias, Universidad Nacional de Santiago del Estero, Avda, Belgrano (S) 1912, 4200, Santiago del Estero, Argentina
[b] Departamento de Química Orgánica, Facultad de Ciencias Químicas, Universidad Nacional de Córdoba, Agencia postal 4, Casilla 61, 5000, Córdoba, Argentina

ARTICLE INFO

Article history:
Received 9 December 2009
Received in revised form 6 May 2010
Accepted 8 May 2010
Available online 15 May 2010

Keywords:
Hydrogenation
Chalcones
Hydrogen permeating
Palladium electrode
Selective reduction

ABSTRACT

The hydrogenation of benzalacetone and benzalacetophenone was carried out using atomic hydrogen permeating through a palladium membrane. A two-compartment cell separated by a Pd sheet or a palladized Pd (Pd/Pd black) sheet electrode was employed. The reduction products were identified by (GC) gas chromatography, UV–vis absorption spectroscopy and NMR spectroscopy. The carbon–carbon double bond was hydrogenated and the benzylacetone and benzylacetophenone were obtained as products using palladium catalyst. The current efficiency for hydrogenation reaction increases when the current density for water electrolysis decreases and depends on the initial chalcone concentration. It is over 90% at the concentration of 10 mmol L^{-1}. The hydrogen absorption and diffusion into and through a palladium membrane electrode has been studied by using an electrochemical impedance spectroscopy method. The impedance results would indicate that the hydrogen permeated through the membrane is consumed by the chalcone during the hydrogenation process keeping as the permeable boundary condition in the outer side of the Pd membrane the hydrogen activity almost zero. The hydrogen entering the metal through an adsorbed state and the rate of hydrogen absorption is diffusion-controlled.

1. Introduction

Chalcones are α,β-unsaturated ketones, which have four possible substituents: R1, R2, R3 and R4. R1 is the substituent in the Cα, in the Cβ and R4 is directly bound to the carbonyl group (Fig. 1). In benzalacetone, the substituent R1 is a phenyl (C_6H_5) group and R_4 a methyl group; while, in benzalacetophenone both R1 and R4 are C_6H_5 groups. Some chalcones are open chain flavonoids whose basic structure includes two aromatic rings connected by an α,β-unsaturated carbonyl group. They are usually obtained from natural products with extractive techniques [1–3] or by several homogeneous [4,5] and heterogeneous [6,7] synthetic methods. The importance of these chalcones is due to their wide range of biological and chemical properties.

Reduction reaction of α,β-unsaturated carbonyl compounds [8] can occur in different ways. It may lead to different products such as (a) an allylic alcohol, resulting from the attack of an hydride the carbonyl group, (b) a saturated carbonyl compound, resulting from the hydrogenation of the carbon–carbon double bond and (c) a saturated alcohol resulting from the reduction of the carbon–carbon double bond as well as the carbonyl group [9]. The most common hydrogenation catalysts are transition metals. On metals the reactivity of isolated C=C bond is always higher than that of C=O bonds and this behavior is likely related to the bond adsorption strength [10]. Palladium is a very good catalyst for the C=C hydrogenations, but a very bad catalyst for hydrogenation of carbonyl compounds. It is known that this is due to a too weak adsorption of carbonyls under reaction conditions. On the other hand, the selective hydrogenation of the α,β-unsaturated ketones to obtain the corresponding unsaturated alcohols need the activation of the carbonyl group which is less reactive than the olefinic bond. Modified metal with cation [11], single crystals [12], polycrystalline nanoparticles and orientated nanoparticles supported on carbon are employed for the hydrogenation of α,β-unsaturated compounds [13]. Santori et al. [14] investigated the behavior of Pt/SiO_2 and tin-modified Pt catalysts, in the hydrogenation of aromatic ketones such as acetophenone, 3,4-dimethoxyacetophenone, benzophenone and chalcone. The different catalysts used led to high selectivity values of the desired products.

The electrocatalytic hydrogenation (ECH) is one of those methods which have been used since the beginning of the last century [15]. The active hydrogen is produced in powdered cathodes, particularly on Raney-nickel or palladium over carbon catalysts. The outset is similar to the catalytic hydrogenation (CH) where unsaturated molecules as well as hydrogen atoms are adsor-

* Corresponding author. Tel.: +54 385 4509528; fax: +54 385 4222595.
E-mail addresses: mcgutier@unse.edu.ar (M. Gutierrez), bmishima@unse.edu.ar (B.A. López de Mishima).

0013-4686/$ – see front matter © 2010 Elsevier Ltd. All rights reserved.
doi:10.1016/j.electacta.2010.05.032

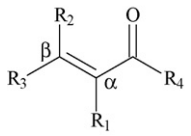

Molecule	R_1	R_2	R_3	R_4
Benzalacetophenone	H	H	C_6H_5	C_6H_5
Benzalacetone	H	H	C_6H_5	CH_3

Fig. 1. Scheme of chalcones.

bed on the catalyst surface. However, the catalytic hydrogenation frequently needs high temperature and pressure to sustain the process. In the electrocatalytic method, the H_{ads} is produced by the proton discharge onto surface sites. Thus, the advantage of the electrocatalytic method is the *in situ* generation of atomic hydrogens on the surface of the electrode, which can be directly used for the envisaged hydrogenation. Several techniques were developed to improve the electrocatalytic hydrogenation [16]. The electrocatalytic method was also employed on the chalcone reduction reaction in early research performed by a Russian group [17]. They studied the reduction of benzalacetophenone at a platinized platinum (Pt/Pt) electrode in dioxane-sulfuric acid solution. Chromatographic analysis disclosed that dihydrochalcone was formed during electrolysis. Recently, Calvo et al. demonstrated the good agreement between electrocatalytic hydrogenation method and heterogeneous catalysis [18]. They performed the hydrogenation of ethyl pyruvate to yield S-ethyl lactate over palladium supported on carbon felt electrodes modified with cinchonidine. Their results were in good agreement with previously reported heterogeneous enantioselective hydrogenation on Pd/C catalyst using molecular hydrogen at high pressure. The ECH limitation is the requirement of a large surface of the catalyst employed as working electrode and the need of adding a supporting electrolyte that often leads to difficulties with subsequent product purification procedures.

Inoue et al. have developed a new hydrogenation system using a two-compartment cell separated by a Pd sheet with a thickness of 50 μm [19]. This system was composed of three processes, which were the following: (i) the electrochemical production of atomic hydrogen by water electrolysis on one side of the Pd sheet, (ii) permeation of the atomic hydrogen through the Pd sheet and (iii) hydrogenation on the other side. The water electrolysis and the hydrogenation reaction proceed on different sides of the metal sheet. As a consequence, it is not necessary to separate the supporting electrolyte from the products. The method was used for hydrogenation of styrene [19], 4-methyl styrene [20], in the hydrogenolysis of the azo dye amaranth [21] and in the dechlorination of 4-chlorotoluene [22]. To the best of our knowledge, this system has never been assayed with chalcones.

The hydrogenation process would be described as follows [22]: in the electrolytic reduction of water at one side of the Pd sheet electrode in alkaline solution, one-electron reduction of the water molecule occurs

$$H_2O + M + e^- \rightleftarrows MH_{ad} + OH^- \quad (1)$$

where MH_{ad} represents an hydrogen atom adsorbed on the Pd sheet. Most of H_{ad} atoms diffuse into the Pd sheet at a velocity proportional to their concentration gradient to reach the other side of the Pd sheet.

$$H_{ad}\ (\text{side } 1) \rightleftarrows H_{ab} \quad (2)$$

where H_{ab} represent the absorbed hydrogen. Permeated hydrogen atoms via an adsorption step at the other side are utilized as the hydrogen source for the hydrogenation of organic molecules.

$$H_{ab} \rightleftarrows H_{ad}\ (\text{side } 2) \quad (3)$$

$$Y_{ad} + 2H_{ad}\ (\text{side } 2) \rightleftarrows H_2Y \quad (4)$$

In the present work the hydrogenation of benzalacetophenone and benzalacetone is performed using atomic hydrogen permeating through a Pd and modified palladized Pd sheet electrode. The objective is to optimize the hydrogenation method using simple chalcones to obtain exclusively dihydrochalcones as reaction products. After that, the optimized permeating method will be assayed with more complex molecules as naringin chalcone and neohesperidine chalcone. They are glycosilated flavanons and their corresponding dihydrochalcones present important properties as sweeteners [23]. Neohesperidin dihydrochalcone (NHDC) is a safe semi-synthetic low-calorie sweetener, bitterness blocker, and flavor enhancer with unique properties and applications for the food, beverage, pharmaceutical, and animal feed industries.

2. Experimental

2.1. Chalcone preparation

The benzalacetophenone (1,3-diphenyl-2-propen-1-one) and the benzalacetone (4-phenyl-3-buten-2-one) were obtained by the condensation of acetophenone or acetone with benzaldehyde in the presence of aqueous alcoholic alkali (method of Claisen-Schmidt) [24]. An aliquot corresponding to 1.1 mol of acetone was mixed with 0.4 mol of benzaldehyde. An aliquot of 10% NaOH aqueous solution was added and the temperature was controlled with a cold bath in the range of 25–31 °C. Hydrochloric acid was added up to neutralization and the aqueous layer was extracted with benzene. The product formed was recrystallized from ethanol. The benzalacetophenone was prepared using a similar method. The corresponding moles of acetophenone and benzaldehyde were added to a NaOH water–ethanol solution previously cooled on an ice bath. The temperature was controlled in a range between 15 and 30 °C.

The melting point of the purified benzalacetophenone obtained was 54–56 °C and the benzalacetone melting point was 40–42 °C. Both ranges are in good agreement with the literature values [24]. These chalcones were also characterized by using UV–vis and ^1H and ^{13}C NMR analysis. The spectra obtained are described in Section 3 of the present paper. The benzalacetophenone and benzalacetone solutions for hydrogenation reactions were prepared using ethanol as solvent.

2.2. Cell and equipment

The cell used for the catalytic hydrogenation was composed of two compartments separated by a Pd sheet (geometric area: 3.14 cm^2, thickness: 50 μm) which served as a cathode for water electrolysis in 1 mol L^{-1} KOH aqueous solution to produce atomic hydrogen [25]. A platinum sheet was used as a counter electrode. The galvanostatic electrolysis was carried out at various applied currents between 25 and 150 mA.

No supporting electrolyte was needed by using this hydrogenation method and the benzalacetone and benzalacetophenone solutions were prepared in ethanol solvent and the concentration range was from 0.1 to 10 mmol L^{-1}. As chalcones are photosensitive compounds, their degradation induced by light was prevented. The cell compartment containing the chalcone solution was protected from light action with aluminum foil and adequately closed to prevent solvent evaporation and the consequent concentration changes. Chalcones remained un-reacted in the absence of the hydrogenation conditions. Their stability was monitored for 25 h, a time period equivalent to that used in the experiments. This stability was verified by GC and by UV spectrophotometry.

For enhancing the catalytic activity for the hydrogenation, the load of the catalysts (palladium) on the Pd sheet electrode must be effective.

Therefore, the Pd sheet was palladized using the permeating hydrogen method. For the palladization method the same two-compartment cell was used. A 1 mol L^{-1} KOH solution was put in the compartment having a Pt sheet anode and a Pd cathode for the production of active hydrogen. A 1 mol L^{-1} HCl solution containing 25 mmol L^{-1} $Pd(NH_3)_6Cl_2$ was introduced into the other compartment for the deposition of Pd black. The active hydrogen was produced in galvanostatic electrolysis at 3.4 mA cm^{-2} for 60 min.

A potenciostat-galvanostat L.Y.P. ELECTRONIC M10, controlled with software was used for the water electrolysis.

The course of the hydrogenation reaction was followed by UV–vis absorption spectroscopy (UNICAM scanning spectrometer UV-2) as well as Gas chromatography (GC). The GC measurements were performed in a Konik HRGC 3000 C Chromatograph, coupled with a Konikron data analysis programmer equipped with a capillary column Kromxpek DEGS 15% and FID detector.

The reaction product purification was carried out by a chromatographic separation on silicagel plates using a radial chromatograph and a mixture of hexane–ethyl acetate (95:5) as elution solvent system revealed with UV light. Three pure compounds were obtained. The purity of such compounds was checked by thin layer chromatography and gas chromatography. The reaction product identification was performed by NMR measurements.

^1H NMR spectra were measured in $CDCl_3$ with TMS as internal standard at 200.13 MHz on a Bruker AC 200 NMR spectrometer [26]. Chemical shifts (relative to TMS) are expressed in ppm and coupling constant (J) in Hz.

2.3. Determination of real area and roughness factor

The real area and roughness factor of the sheet Pd electrode and palladized Pd (Pd/Pd black) electrode were determined by linear sweep voltammetry [27,28]. A palladium electrode previously reduced at 0.0 V was potentiostated at 1.0 V in oxygen saturated 0.1 mol L^{-1} KOH solution for 120 s and then the potential applied to the electrode was linearly scanned at 20 V s^{-1} to −0.20 V at which the adsorbed oxygen species were considered to be completely reduced. The amount of charge required to reduce the adsorbed oxygen species, Q_{red}, was calculated by graphic integration of the current-potential response. The values of palladium sheet and Pd/Pd black electrodes were found to be about 1875 and 3541 μC, respectively. Taking the charge density value of 255 μC cm^{-2} required to complete coverage with oxygen adsorbed species the real area and roughness factor were calculated [29]. The roughness factor is the relation between real area and the geometric area. The values of the Pd sheet and Pd/Pd black specimen were calculated to be 2.3 and 4.4, respectively. The roughness factor of the sheet Pd specimen was close to that values of 2 and 2.2 reported by other researchers [28,30].

All the values of the density current informed in the present paper were calculated by considering the real area of the palladium electrodes.

2.4. Chemical hydrogenation

The chemical reduction of benzalacetophenone and benzalacetone by a typical catalytic hydrogenation for the identification of the products was done. The procedure was carried out in catalytic reduction equipment at 2 atm of H_2 pressure using 0.001 g of platinum black as catalyst and 50 cm^3 of a 10 mmol L^{-1} benzalacetophenone (or benzalacetone) ethyl acetate solution [27].

2.5. Electrochemical impedance spectroscopy

The impedance measurements were used with permeation cell for analyzing the hydrogen permeation. A cathodic potential was imposed to the cathodic side of the palladium membrane by using an AUTOLAB-PGSTAT 30. The hydrogen absorbed into the cathodic side of the membrane diffuses toward its anodic side. The electrode impedance was determined using a Frequency Response Analyzer System (FRA) module by superimposing an ac signal of 5 mV amplitude on a dc potential of −0.60 to −0.70 V (*rhe*) over the frequency ranging from 10 mHz to 10 kHz. The experimental frequency was scanned from high to low value. All experiments were carried out at room temperature.

3. Results and discussion

3.1. Hydrogenation of chalcones by the permeation method

The benzalacetophenone and benzalacetone hydrogenation reactions were followed by UV–vis absorption spectroscopy. Fig. 2 shows the typical absorption spectrum between 220 and 400 nm of a 0.1 mmol L^{-1} benzalacetophenone ethanolic solution. The initial spectrum shows an absorption band with a λ_{max} at 310 nm. The major adsorption band in chalcones (Band I) usually occurs in the range of 340–390 nm but this absorption band shifts to shorter wavelengths in chalcones lacking an oxygenated B-ring [31]. In this sense, benzalacetophenone λ_{max} of 310 nm is in agreement with the literature.

The benzalacetophenone solution was put in one of the compartment of the cell and exposed to active hydrogen for 25 h with a Pd sheet electrode. The current density for the electrogeneration of the hydrogen atoms was 3.4 mA cm^{-2}. The band at 310 nm decreases during the hydrogenation process. Similarly, the benzalacetone solutions presented the absorption λ_{max} at 288 nm and the spectral behaviour during the hydrogenation reaction was similar to that of the benzalacetophenone solution.

For enhancing the catalytic activity for the chalcones hydrogenation, palladium was deposited on the substrate side of the Pd sheet using atomic hydrogen permeating through it, as described in Section 2.

The rate of the hydrogenation reaction was evaluated for both two Pd electrodes: Pd sheet and palladized Pd measuring the absorbance at λ_{max} value as a function of time. Fig. 3 shows the absorbance values of benzalacetophenone solution at 310 nm when a density current of 3.4 mA cm^{-2} was used for the production of the H atoms. The time-dependent absorbance A_t was fitted using a first-order kinetic law at the monitored wavelength, as shown in Eq. (5)

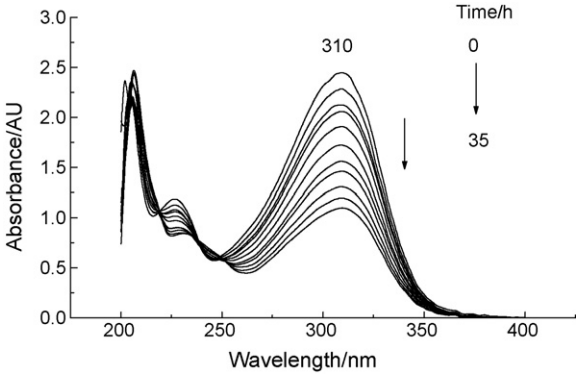

Fig. 2. UV–vis absorbance spectral changes during the hydrogenation process of 0.1 mmol L^{-1} benzalacetophenone methanolic solution. The current for the electrogeneration of active hydrogen was 3.4 mA cm^{-2} for 35 h.

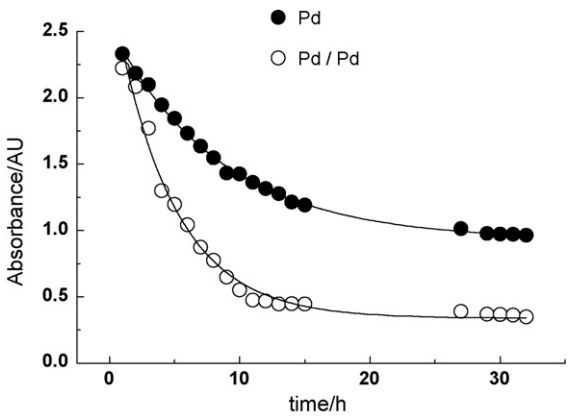

Fig. 3. Time course of the benzalacetophenone solution absorbance for two kinds of electrodes: Pd sheet and Pd/Pd black. The initial concentration was 0.1 mmol L^{-1} and the current for producing atomic hydrogen was 3.4 mA cm^{-2}.

[32].

$$A_t = A_\infty + (A_0 - A_\infty)\exp(-k_{obs}t) \quad (5)$$

where A_0 and A_∞ are the absorbance values at the initial and final times of the reaction, respectively, and k_{obs} is the observed first-order rate constant that included the active hydrogen concentration. The rate constants were estimated from the experimental results of Fig. 2 and the values for the Pd sheet and Pd/Pd black electrodes were 0.12 and 0.22 h^{-1}, respectively. The increase of rate constant values is in agreement with the increase of roughness factor, which changes from 2.3 for the Pd sheet electrode to 4.4 for the Pd/Pd black electrode. The real area and roughness factor were calculated from the amount of charge required to reduce the adsorbed oxygen species, Q_{red} and taking the charge density value of 255 μC cm^{-2} required to complete coverage with oxygen adsorbed species as described in the experimental section. Therefore, the palladized Pd electrode improved the rate of the benzalacetophenone hydrogenation as a result of the active area increased as expected in these conditions. The H atoms permeate no only through the Pd sheet but also through the Pd black deposits. As previously reported [20], the effect of roughness factor over the 4-methylstyrene hydrogenation indicates that the product formation rate increased with an increase in surface roughness factor until this increase was suppressed steadily, suggesting that the rate-determining step changed from the hydrogenation to the supply of the active hydrogen.

The hydrogenation of the chalcone solutions was performed at different currents for the production of active hydrogen on Pd/Pd black electrode. Fig. 4a shows the absorbance values as a function of time for benzalacetophenone solution in the galvanostatic electrolysis at various applied currents. The disappearing rate of benzalacetophenone during the hydrogenation process increases with the current value.

Fig. 4a inset also shows the rate constant values of the benzalacetophenone reaction calculated from Eq. (5) as a function of the current density for the production of atomic hydrogen. The reduction rate increases almost linearly with an increase in the current density up to 8.6 mA cm^{-2}. This result indicates that the current efficiency for the reduction of benzalacetophenone is almost constant in the range of current density from 3.4 to 8.6 mA cm^{-2}. While higher values deviate from the linear behavior. These results would suggest that the amount of active hydrogen limits the hydrogenation process. On the other hand, the hydrogen absorption reaction *(har)* at the input side of Pd membrane competes with the hydrogen evolution reaction *(her)* which decreases the permeation yield. In this sense, Gabrielli et al., working with Pd membranes of 50 and 100 μm thicknesses, informed that a permeation yield close to 100% is obtained when the current density is lower than 2 mA cm^{-2}. Beyond this value, the *har* competes with the *her* and the hydrogen atoms generated at the input side by applied current, is partially inserted in the palladium membrane and partially evolved as H_2 [33].

The current efficiency for the hydrogenation of benzalacetophenone was evaluated for two independent methods as follows: (i) dividing the value of the specific rate of benzalacetophenone disappearing (the slope of each straight line in Fig. 4a) by that calculated from the charge passed during the reaction time, (ii) dividing the value of the product yield by the charge that corresponds to the hydrogen generated during the reaction hydrogenation time (25 h). The identification of the products is explained farther on in the separated item. The current efficiency increased when the current density for water electrolysis decreased. The maximum value was 31% and corresponds to 3.4 mA cm^{-2}. This behavior is similar to the dechlorination of 4-chlorotoluene by palladized Pd electrode [22] and the efficiency value is in agreement with the results informed for the discoloration of amaranth using Pd/Pd black electrode and a low initial concentration value [21].

The effect of the initial chalcone concentration on the current efficiency is shown in Fig. 4b. In the same figure, the values of the hydrogenation efficiency calculated from the product yield determined by chromatographic method are included indicating that there is a good agreement. The current efficiency increased almost linearly with an increase in the initial benzalacetophenone concentration until 1.5 mmol L^{-1}. Beyond such concentration, the values were deviated, the current efficiency at 10 mmol L^{-1} concentration being of 97%. This value suggests that the produced hydrogen atoms are effectively used in the hydrogenation of chalcone and the amount of active hydrogen could limit the hydrogenation process. To support this hypothesis, the Devanathan and Stachurski method carried out by Inoue et al. would be used as the conventional method. Inoue et al. evaluated the rate of hydrogen permeation for Pd/Pd black electrode for a similar hydrogenation system measuring the anodic current for the oxidation of permeated H atoms through the Pd membrane of 50 μm thickness. The oxidation current increased continuously with the time after initiation of the galvanostatic electrolysis for the production of H atoms and then, it reached a saturation limit because the H atom permeation reached a steady state [25]. Therefore, they concluded that hydrogenation process can be limited by the active hydrogen. As an innovative alternative to study the hydrogen permeation during the hydrogenation reaction, the electrochemical impedance spectroscopy (EIS) method was proposed in this work. EIS allows to estimate the hydrogen diffusion coefficient and to distinguish the different elementary steps of the reaction.

3.2. Electrochemical impedance spectroscopy

The permeation experiments with EIS were carried out by imposing a cathodic potential on the entry side to produce hydrogen, which enters the metallic membrane. When the hydrogen permeates to the opposite face of the membrane, it can be used for the hydrogenation reaction. The outside is under open circuit potential. Fig. 5a shows the Nyquist plots of impedance spectra for the Pd/Pd electrode in 0.1 mol L^{-1} NaOH solution in the potential range of −0.60 to −0.70 V in the entry side and 0.1 mmol L^{-1} chalcone ethanolic solution in the outer side.

The impedance spectra involve charge transfer, adsorption and absorption reactions, as well as diffusion in the electrode in sequence as the frequency decreases. The semicircle in the high frequency range corresponds to the charge transfer reaction. Warburg impedance appears in the low frequency range, represen-

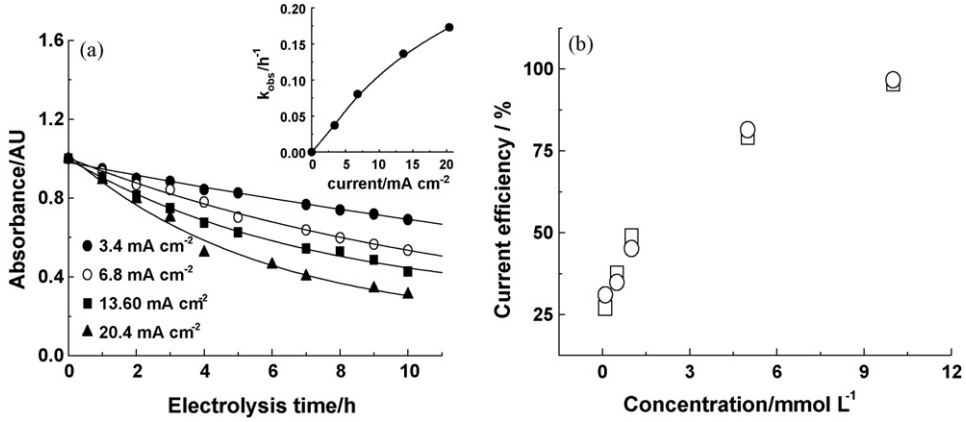

Fig. 4. Effect of the current for active hydrogen electrogeneration and solution concentration in the benzalacetophenone hydrogenation reaction. (a) Absorbance vs. time, inset, k_{obs} calculated from Eq. (5) as a function of the density current. (b) Current efficiency as a function of initial concentration calculated from slopes (□) and the product yields (○). Current for producing atomic hydrogen: 3.4 mA cm^{-2}.

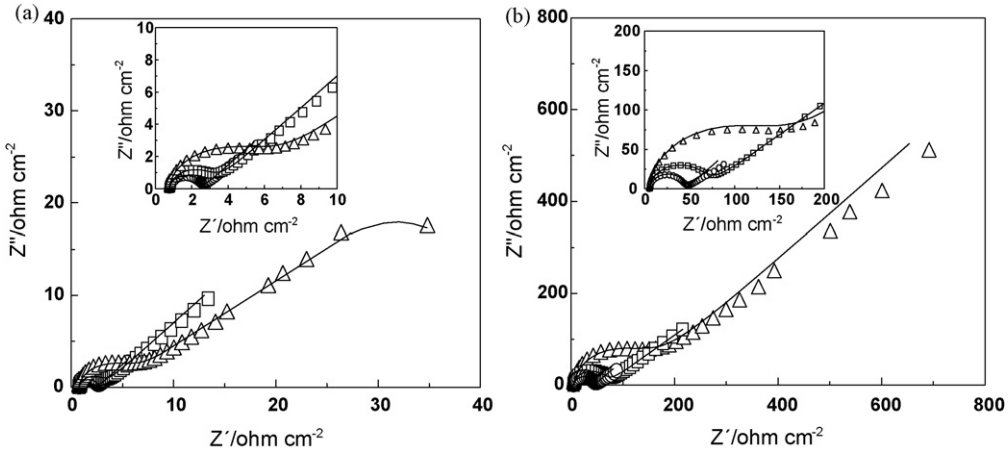

Fig. 5. Impedance complex plot obtained from Pd electrode at various potential of (△) −0.60 V, (□) −0.65 V, (○) −0.70 V. Solid line represents the simulated curves calculated by using optimum fitted parameters: (a) 0.1 mol L^{-1} KOH in the entry side compartment of the permeating cell and 0.1 mmol L^{-1} benzalacetophenone solution in the outside compartment; (b) 0.1 mol L^{-1} KOH in the two compartments permeating cell.

ting the diffusion process of hydrogen under permeable boundary conditions. When the potential decreases, the Warburg impedance deviates more negatively from the theoretical curve and the semicircle is smaller.

Real and imaginary components, Z' and Z'', obtained at each dc potential were analyzed by using CNLS fitting method to determine the kinetic parameters.

We considered the permeable boundary condition for hydrogen permeation [29]. In alkaline solutions, the hydrogen discharge shows the hydrogen evolution reaction (*her*) and the hydrogen absorption reaction (*har*). The first step of the *her* involves an electroreduction of the water molecule, with the formation of hydrogen adsorbed on the metal surface (Volmer adsorption), followed by either Tafel chemical desorption or Heyrovsky electrochemical desorption [34].

The *har* is described by two models. One is indirect *har*, that is hydrogen entering the metal through an adsorbed state [35]. The other is direct *har*, that is hydrogen directly entering the metal without passing through the adsorbed state [36]. Both *her* and *har* compete on the Pd electrode.

We considered the indirect model and the constant phase element (*cpe*) in the double-layer impedance. The equations used are:

$$Z_{\mathrm{CPE}} = \frac{1}{B_0(j\omega)^{\varphi}} \tag{6}$$

where B_0 is a constant having dimension of F cm^{-2} s$^{-(1-\varphi)}$ [37,38]. Thus, the total impedance is

$$Z_t = R_s + \frac{1}{B(j\omega)^{\phi} + Y_f} \tag{7}$$

where R_s is the solution resistance.

The values of the parameters obtained from the fitted one are summarized in Table 1. From these values theoretical impe-

Table 1
Optimum fit-parameters involved in Eq. (8) obtained at various overpotentials.

E vs. Hg/HgO (V)	B_0 ($\times 10^4$ F cm^{-2} s$^{-(1-\varphi)}$)	φ ($\times 10^{-1}$)	R_{ct} (Ω cm^2)	B' ($\times 10^5$ cm s^{-1})	I_{eq} ($\times 10^4$ cm)	D_H ($\times 10^7$ cm^2 s^{-1})
−0.60	2.04	9.72	130.1	182.4	11.2	3.1
−0.65	1.98	9.32	52.2	45.2	4.1	3.5
−0.70	1.97	9.38	11.1	13.5	3.2	3.6

dance complex are obtained which are represented by solid lines in Fig. 5a.

The equilibrium constant K_{eq} for the *har* is the concentration ratio between absorbed hydrogen to the adsorbed hydrogen on the surface and it is the inverse of the l_{eq} informed in Table 1. The K_{eq} values were found to be: $8.9 \times 10^2\ cm^{-1}$ at −0.70 V, $2.4 \times 10^3\ cm^{-1}$ at −0.65 V and $3.1 \times 10^3\ cm^{-1}$ at −0.60 V. The values of K_{eq}, the charge transfer resistance, R_{ct}, and the hydrogen diffusion coefficient, D_H, are in agreement with those informed by Lim and Pyun [29]. They worked with permeation cell where the cathodic potential was imposed to the cathodic side of the Pd membrane of 50 μm thickness. The anodic side was subjected to a constant anodic potential which allowed any hydrogen to be oxidized to H^+ coming through the membrane, keeping the activity of hydrogen at zero.

Fig. 5b shows the Nyquist plots of impedance spectra for the Pd/Pd electrode in 0.1 mol L^{-1} NaOH solutions in two compartment of the cell (without chalcone), at −0.60, −0.65 and −0.70 V. In this case, the hydrogen does not cross the metal solution interface at the exit side. The complex diagram shows that the Warburg impedance is not deviated with decreasing potential as it is observed in Fig. 5a with the presence of chalcone. Besides, the vertical capacitive branch for low frequency characteristic of the impermeability conditions does not appear. Gabrielli et al. observed such behaviour for the transfer functions measured at a galvanostatic control of the exit side ($I_2 = 0$) for a 50-μm thickness membrane at a frequency lower than 10 mHz [33]. It is possible that we could not reach such condition because 10 mHz was the lowest frequency value used in our experiments. The results obtained under 10 mHz were not reproducible due mainly to high background noise at low frequencies.

The impedance results obtained during the chalcone hydrogenation process would indicate that the hydrogen permeated trough the membrane is consumed by the chalcone during the hydrogenation reaction keeping the condition of hydrogen activity almost zero in the outer side of the Pd membrane. In our experiment, this side is under open circuit potential conditions. The reaction sequence of the process is the reaction (1) followed by this mechanism [29].

$$MH_{ads} \rightleftarrows MH_{abs} \rightarrow \text{diffusion} \rightarrow MH_{ads} + MY_{ads} \rightarrow H_2Y + 2M \quad (8)$$

where MY_{ads} and MH_{ads} represents the chalcone molecules and hydrogen atom adsorbed on the metal surface in the other side. The hydrogen absorption rate is diffusion-controlled.

3.3. X-ray diffraction

Fig. 6a shows the X-ray diffractograms recorded for Pd metal sheet before being used in the hydrogenation process. The (1 1 1), (2 0 0) and (2 2 0) peaks relative to palladium *fcc* structure are observed. The relative intensity of the (1 1 1) peak is lower than those of (2 0 0) and (2 2 0) peaks, showing same preferential orientation in the crystalline structure of Pd sheet. Fig. 6b shows the X-ray diffraction patterns for Pd/Pd obtained after the hydrogenation process of the chalcone at 6.8 mA cm^{-2}. It shows the same pattern of peaks of the Pd sheet diffractogram with different intensities and the spectrum is similar to that informed in the literature. The palladized process performed with hydrogen permeating method produces a Pd black deposit [39]. The (1 1 1) peak is higher than Pd sheet and there are no peaks corresponding to hydride formation. In both figures, the peaks corresponding to palladium oxide were not observed. The lattice parameters were calculated from the Bragg equation and the values are in agreement with the literature being 3.90 for Pd sheet and 3.89 for Pd/Pd sample [40].

SEM photographs of surface for the Pd sheet and Pd/Pd black samples are shown in Fig. 7a and b, respectively. The surface of Pd sheet is smooth with some defects while the surface of Pd/Pd black shows a three-dimensional growth of Pd black deposits with a crystallite size of about 1 μm. After hydrogenation reaction the attack of the surface is also observed.

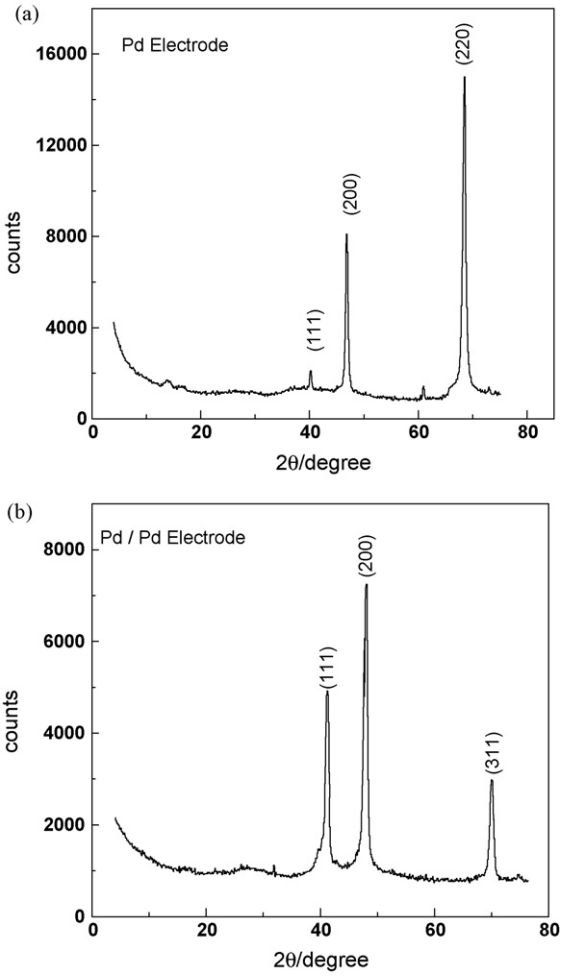

Fig. 6. XRD diffraction pattern for Pd electrode: (a) Pd sheet before permeation reaction; (b) Pd palladized on Pd sheet electrode after using in hydrogen permeation reaction.

3.4. Identification of reaction products

The reaction mixture of hydrogenation products was analyzed by gas chromatography. The purification of the hydrogenated products was carried out by radial chromatography, and subsequent identification of them by RMN spectroscopy.

The benzalacetophenone (1,3-diphenyl-2-propen-1-one) is and α,β-unsaturated aromatic ketone. Hydrogenation of the double bond C=C produces a 1,3-diphenyl-propan-1-one (**1a**); if the C=O is hydrogenated, a 1,3-diphenyl-2-propen-1-ol (**1b**) is formed; and subsequent hydrogenation of either product leads to a 1,3-diphenyl-propan-1-ol (**1c**) (Fig. 8).

The main hydrogenation products were also produced by the classical catalytic hydrogenation (CH). Benzalacetophenone were hydrogenated using hydrogen at high pressure and black platinum catalyst as described in the experimental section. The chemical hydrogenation products were separated using radial chromatography and subsequently, NMR analysis for each isolated fraction was performed for identifying the compounds. After that these fractions were analyzed by GC and used as standard for identification purposes.

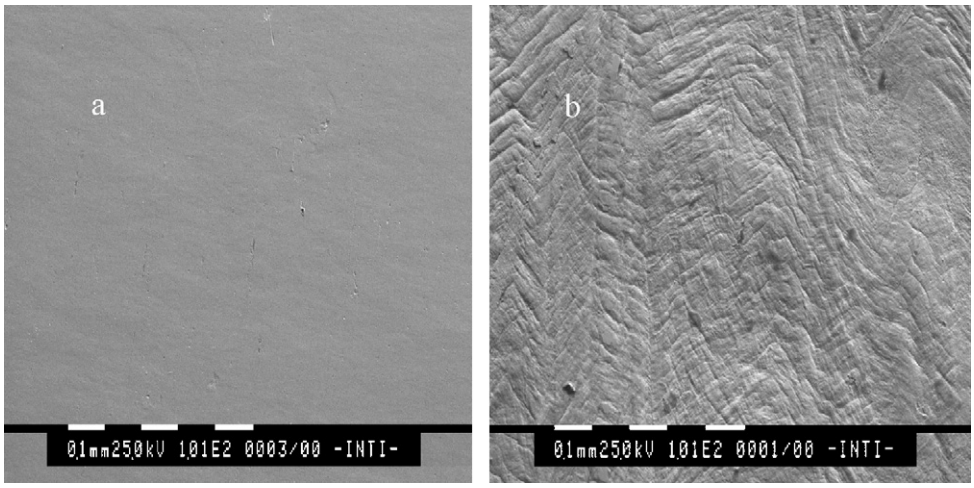

Fig. 7. SEM images of Pd electrode: (a) Pd sheet before permeation reaction; (b) Pd palladized on Pd sheet electrode after used in hydrogen permeation reaction.

3.5. Benzalacetophenone NMR analysis

The spectrum of ^{1}H NMR of the *E*-chalcone synthesized in the laboratory was coincident with that published in the literature [41]. After chemical CH, the signal of H of benzalacetophenone (**1**) and the reduction products (**1a**), (**1b**) and (**1c**) are observed (Fig. 8). The spectrum shows two triplets at $\delta = 3.30$ ppm ($J = 7.8$ Hz) and $\delta = 3.07$ ppm ($J = 7.8$ Hz) assigned to the hydrogen of position 2 and 3 of the 2,3-dihydrochalcone (**1a**), respectively, which is the main product. Traces of the products (**1b**) and (**1c**) are present: a triplet at $\delta = 4.65$ ppm ($J = 7.8$ Hz) and a doublet at $\delta = 5.40$ ppm, respectively. The relationship obtained from the integration of the (**1**) and (**1a**) signal compounds is 7.9/2.1 (a ratio of 3.76). The result indicates that compound (**1a**), benzylacetophenone yield corresponds to a 79%, and the (**1b**) (**1c**) are in traces. The benzalacetophenone remains in 21%.

The hydrogen permeation reaction was carried out and the products were analyzed by GC and identified using the product of chemical hydrogenation as standard. Only one product was observed, which was identified as (**1a**) benzylacetophenone (86%). The benzalacetophenone remains in 14%. Relative changes were evaluated assuming that the consumption of the chalcone was due only to the formation of hydrogenated product by permeation method.

Fig. 9 shows the chromatogram of the benzalacetophenone solutions: (a) benzalacetophenone before the reaction (b) after hydrogenation process using CH method and (c) after hydrogen permeation reaction. The benzalacetophenone shows a peak at $t_R = 8.4$ min. After the reaction, three peaks corresponding to the products produced by CH method are observed at $t_R = 5.4$ min, $t_R = 5.6$ min and $t_R = 5.9$ min and one peak of the product for permeating method at $t_R = 5.6$ min.

The hydrogenation reaction for benzalacetone (4-phenyl-3-buten-2-one) using the both methods: chemical and hydrogen permeating through a palladium membrane showed the same behaviour.

The result indicates that compound benzylacetone (4-phenyl-2-butanone) yield corresponds to a 59%, the 4-phenyl-3-buten-2-ol to a 16% and 4-phenyl-2-butanol in 4.5%. The benzalacetone remains in 20.5%.

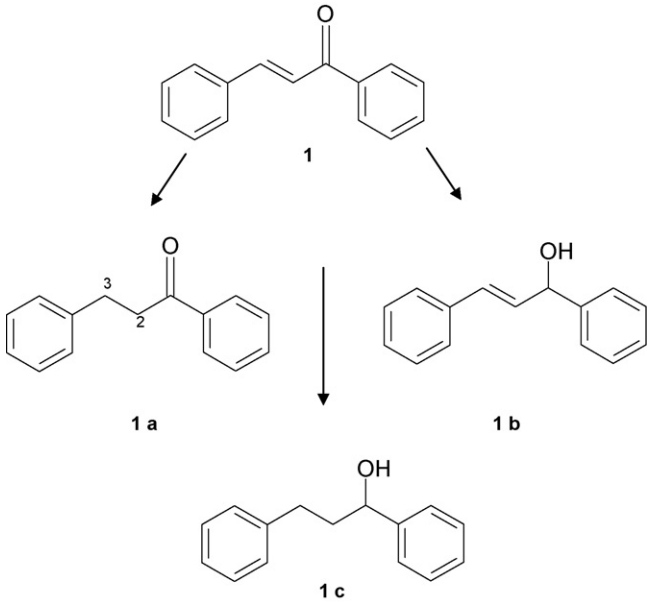

Fig. 8. Scheme of the products obtained in the hydrogenation catalytic reaction of the benzalacetophenone.

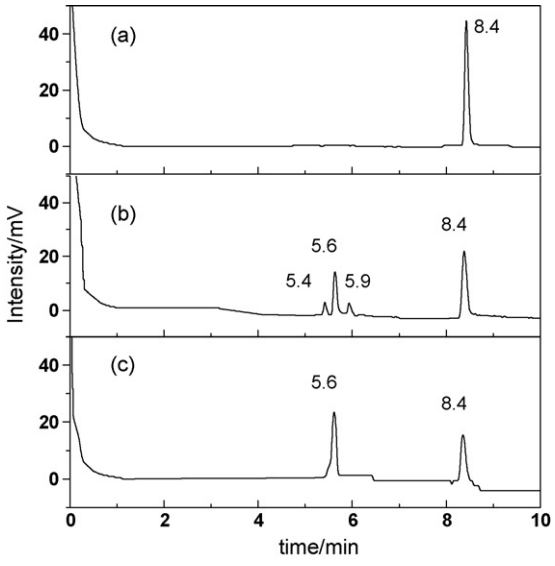

Fig. 9. GC chromatograms of the benzalacetophenone and the hydrogenation reaction products: (a) benzalacetophenone as-synthesized; (b) chemical hydrogenation with gas hydrogen at 2 atm with Pt black as catalyst; (c) hydrogen permeating through Pd/Pd black electrode.

The hydrogen permeation reaction was carried out and the products were analyzed by GC and identified using the product of chemical hydrogenation as standard. Only one product was observed, which was identified as benzylacetone (71%). The benzalacetone remains in 29%.

The results obtained during the catalytic hydrogenation reaction of benzalacetophenone and benzalacetone on Pt/Pt catalyst show that ketone hydrogenated, unsaturated alcohol and saturated alcohol are obtained as products. On the other hand the hydrogenation of these chalcones using permeation hydrogen lead to the ketone hydrogenated as only product. The hydrogen reaction is performed on palladium and Pd/Pd black catalysts and also is a catalytic reaction but the difference is that it is possible controlling the hydrogenation process with the current value of hydrogen generation.

There are several studies of the selective hydrogenation of the α,β-unsaturated carbonyl compounds in relation with the competitive C=C and C=O adsorption [10–13] and it is generally assumed that the reactive bond is the one involved in chemisorption on the surface. Therefore the problem of selective hydrogenation can be reduced in a first rough approximation to determine the electronic factors which control the adsorption mode of the α,β-unsaturated carbonyl compound.

Benzalacetone has similar structure than cinnamaldehyde and chalcone. All of them contain at least a benzene ring, a carbon–carbon double bond and a conjugated carbonyl group. Cinnamaldehyde is one of the most experimentally studied unsaturated aldehydes and it is used as model for theoretical and experimental studies to the selective hydrogenation of the α,β-unsaturated carbonyl compound. Aldaz et al. [13] the influence of the shape/surface structure of Pt nanoparticles on the selective hydrogenation of crotonaldehyde and cinnamaldehyde has been studied. Pt(1 1 1)/C showed higher selectivities to unsaturated alcohol than Pt(1 0 0)/C and Pt/C samples. Delbeq et al. done a very elucidating paper to explain the behavior of platinum and palladium metal towards the hydrogenation of α,β-unsaturated aldehydes [42]. Their argumentation rest on the hypothesis that the double bond which is first hydrogenated is the one involved in the chemisorption on the surface. The preferred adsorption modes allow one to explain the selectivity observed with different geometry molecules They informed that phenyl ring of the cinnamaldehyde has a non-negligible stabilizing interaction with the surface which explains that the adsorption geometries through the C=C bond are more stable than those through the C=O bond. This is present when the four electron repulsions between the surface and the molecule is small and this is the typical case for a palladium catalyst. Palladium is intrinsically a poor catalyst for selective hydrogenation of the C=O bond of a α,β ethylenic aldehyde. Carbonyl groups are usually hydrogenated over platinum while hydrogenation has not been reported over palladium for aliphatic aldehydes [43,44].

In the present paper we assayed for the first time the permeating method for hydrogenation of chalcones using simple molecules as benzalacetone and benzalacetophenone. The electrochemical impedance spectroscopy (EIS) resulted appropriate method to study and model the hydrogenation reaction.

Further work is under progress in our laboratory on the optimization of the hydrogenation of more complex molecules as naringin and neohesperidine chalcones of biological interests.

4. Conclusions

The hydrogenation of the benzalacetophenone and benzalacetone was developed using permeating hydrogen through the palladium membrane electrode. The reaction was carried out using a two–compartment cell separated by Pd sheet and palladized Pd (Pd/Pd black) sheet electrodes. The catalysts were characterized by XRD and SEM.

XRD studies show that there are no peaks corresponding to hydride formation and the peaks corresponding to palladium oxide are not observed. SEM analysis of the Pd/Pd black samples shows a three-dimensional growth of Pd black deposits with a crystallite size of about 1 μm. After the hydrogenation reaction, the attack to the surface is also observed. The current efficiency for hydrogenation reaction increases when the current density for water electrolysis decreases and depends on the initial chalcone concentration. It is over 90% at the concentration of 10 mmol L^{-1}.

The reduction products were identified by GC chromatography, UV–vis absorption spectroscopy and NMR spectroscopy. The ketone hydrogenated, unsaturated and saturated alcohols are obtained when the catalytic hydrogenation is performed using Pt/Pt electrode. The hydrogen permeating method lead to the ketone hydrogenated as single product because palladium catalyst is a very good catalyst for the C=C hydrogenations, but a very bad catalyst for hydrogenation of carbonyl compounds. In addition, the rate of hydrogenation can be easily controlled by the electrolytic current, which is one of the advantages of that method.

The hydrogen absorption and diffusion into and through a palladium membrane electrode has been studied by using an ac impedance method. We considered the permeable boundary condition for hydrogen permeation and indirect model for *har* that is hydrogen entering the metal through an adsorbed state. The K_{eq}, R_{ct} and D_H values are in agreement with the values informed by Lim and Pyun which worked with permeation cell, where the anodic side was subjected to a constant anodic potential which hydrogen atoms oxidized to H^+ keeping the activity of hydrogen equal to zero. The impedance results obtained in the present paper would indicate that the hydrogen permeated trough the membrane is consumed by the chalcone during the hydrogenation process keeping the hydrogen activity almost zero in the outer side of the Pd membrane.

Acknowledgements

We acknowledge the financial support of CONICET and CICYT-UNSE.

References

[1] J.B. Harborne, T.J. Mabry (Eds.), The Flavonoids Advances in Research, Chapman Hall, London, 1982.
[2] R. Pederiva, J. Kavka, A.T. D'Arcángelo, Ann. Asoc. Quím. Argent. 63 (1975) 85.
[3] D.N. Dhar, The Chemistry of Chalcones and Related Compounds, Wiley, New York, 1981, pp. 201.
[4] G.R. Subbanwad, Y.B. Vibhute, J. Ind. Chem. Soc. 69 (1992) 337.
[5] T. Patonay, Trends Heterocycl. Chem. 3 (1993) 421.
[6] A. Corma, M.J. Climent, H. García, J. Primo, Catal. Lett. 4 (1990) 85.
[7] M.J. Climent, A. Corma, S. Iborra, J. Primo, J. Catal. 151 (1995) 60.
[8] J.G. Handique, A. Purkayashtha, J.B. Baruah, J. Organomet. Chem. 620 (2001) 90.
[9] A.H. McManus, P.J. Guiry, Chem. Rev. 104 (2004) 4151.
[10] V. Ponec, Appl. Catal. A: Gen. 149 (1997) 27.
[11] S. Galvano, A. Donato, G. Néri, R. Petropaolo, Catal. Lett. 8 (1991) 9.
[12] P. Beccat, J.C. Bertolini, Y. Gauthier, J. Massardier, P. Ruiz, J. Catal. 126 (1990) 451.
[13] J.C. Serrano-Ruiz, A. López-Cudero, J. Solla-Gullón, A. Sepúlveda-Escribano, A. Aldaz, F. Rodríguez-Reinoso, J. Catal. 253 (2008) 159.
[14] G.F. Santori, A.G. Moglioni, V. Vetere, G.Y. Moltrasio Iglesias, M.L. Casella, O.A. Ferretti, Appl. Catal. A: Gen. 269 (2004) 215.
[15] R.C.Z. Lofrano, J.M. Madurro, L.M. Abrantes, J.R. Romero, J. Mol. Catal. A: Chem. 218 (2004) 73.
[16] K. Park, P.N. Pintauro, M.M. Baiser, K. Nobe, J. Appl. Electrochem. 16 (1986) 941.
[17] L.A. Taran, S.I. Berezina, L.G. Smolentseva, Y.P. Kitaev, Russ. Chem. Bull. 23 (1974) 2518.
[18] M. Vago, F.J. Williams, E.J. Calvo, Electrochem. Commun. 9 (2007) 2725.
[19] C. Iwakura, T. Abe, H. Inoue, J. Electrochem. Soc. 143 (1996) L71.
[20] H. Inoue, Y. Yoshida, S. Ogata, T. Shimamune, K. Kikawa, C. Iwakura, J. Electrochem. Soc. 145 (1998) 138.

[21] Y. Yoshida, S. Ogata, S. Nakamatsu, T. Shimamune, K. Kikawa, H. Inoue, C. Iwakura, Electrochim. Acta 45 (1999) 409.
[22] H. Inoue, K. Higashiyama, E. Higuchi, C. Iwakura, J. Electroanal. Chem. 560 (2003) 87.
[23] A. Bär, F. Borrego, O. Benavente, J. Castillo, J.A. del Río, Lebensm. - Wiss. und. Technol. 23 (1990) 371.
[24] E.P. Kohler, H.M. Chadwell, Organic Syntheses, vol. 1, Wiley, New York, 1941, p. 78.
[25] Y. Yoshida, S. Ogata, S. Nakamatsu, T. Shimamune, H. Inoue, C. Iwakura, J. Electroanal. Chem. 444 (1998) 203.
[26] M.T. Baumgartner, M.A. Nazareno, M.C. Murguía, A.N. Pierini, R.A. Rossi, Synthesis 12 (1999) 2053.
[27] M.W. Breiter, J. Electroanal. Chem. 81 (1977) 275.
[28] R.V. Bucur, F. Bota, Electrochim. Acta 29 (1984) 103.
[29] C. Lim, S. Pyun, Electrochim. Acta 39 (1994) 373.
[30] L.M. Vracar, D.B. Sepa, A. Damjanovich, J. Electrochem. Soc. 136 (1989) 1973.
[31] I. Ahmad, J.A. Anderson, C.H. Rochester, T.J. Dines, J. Mol. Catal. A: Chem. 135 (1998) 63.
[32] J.H. Espenson, Chemical Kinetics and Reaction Mechanisms, 2nd ed., McGraw-Hill, New York, 1995, pp. 22.
[33] C. Gabrielli, P.P. Grand, A. Lasia, H. Perrot, J. Electroanal. Chem. 532 (2002) 121.
[34] A. Lasia, D. Grégoire, J. Electrochem. Soc. 142 (1995) 3393.
[35] O.M. Bockris, J. McBreen, L. Nanis, J. Electrochem. Soc. 112 (1965) 102.
[36] I.A. Bagotskaya, Zhur. Friz. Khim. 36 (1962) 2667.
[37] J. Brug, A.L.G. van der Eeden, M. Sluyters-Rehbach, J.H. Sluyters, J. Electroanal. Chem. 176 (1984) 275.
[38] J.R. Macdonald (Ed.), Impedance Spectroscopy, J. Wiley, New York, 1987, p. 16.
[39] C. Iwakura, Y. Yoshida, H. Inoue, J. Electroanal. Chem. 431 (1997) 43.
[40] V.M. Azambuja, D.S. dos Santos, L. Pontonnier, S. Miraglia, D. Fruchart, J. Alloys Compd. 346 (2002) 142.
[41] N.M. Glagovich, T.D. Shine, J. Chem. Educ. 82 (2005) 1382.
[42] F. Delbecq, P. Sautet, J. Catal. 152 (1995) 217.
[43] R.L. Augustine, Catal. Rev. Sci. Eng. 13 (1976) 285.
[44] P.N. Rylander, in: A. Methcohn, R. Katrizky, C.W. Rees (Eds.), Hydrogenation Methods Best Synthetic Method (O), Academic Press, New York, 1988, p. 70.